Journal of Solid State Chemistry 185 (2012) 130–135

Contents lists available at SciVerse ScienceDirect

Journal of Solid State Chemistry

journal homepage: www.elsevier.com/locate/jssc

Laser patterning and preferential orientation of two-dimensional planar β-BaB_2O_4 crystals on the glass surface

F. Suzuki, K. Ogawa, T. Honma, T. Komatsu *

Department of Materials Science and Technology, Nagaoka University of Technology, 1603-1 Kamitomioka-cho, Nagaoka 940-2188, Japan

ARTICLE INFO

Article history:
Received 1 September 2011
Received in revised form
2 November 2011
Accepted 3 November 2011
Available online 12 November 2011

Keywords:
Laser-induced crystallization
Planar crystals
β-BaB_2O_4
Second harmonic intensity
Preferential orientation

ABSTRACT

The laser-induced crystallization method is applied to pattern two-dimensional planar β-BaB_2O_4 crystals on the surface of Sm_2O_3–BaO–B_2O_3 glass. By scanning Yb:YVO_4 fiber lasers (wavelength: 1080 nm) continuously with a small step (0.5 μm) between laser irradiated areas, homogeneous planar β-BaB_2O_4 crystals are patterned successfully, and a preferential growth orientation of β-BaB_2O_4 crystals is confirmed from linearly polarized micro-Raman scattering spectrum and second harmonic intensity measurements. It is found that the crystal growth direction is perpendicular to the laser scanning direction. This relation, i.e., the perpendicular relation, is different from the behavior in discrete crystal line patterning, where the crystal growth direction is consistent with the laser scanning direction. The present study proposes the possibility of the control of crystal growth direction in laser-induced crystallization in glasses.

1. Introduction

Laser micro-fabrication in materials is an important technique for the design and fabrication of high technology devices. Laser irradiation to glass has been regarded as a process for spatially selected structural modification and/or crystallization in glass, and laser-induced crystallization techniques have been applied to various glasses in order to pattern functional crystals in glasses [1–20]. For instance, highly oriented $LiNbO_3$ crystal lines have been patterned on the glass surface by laser irradiations [13,20]. Gupta et al. [10] demonstrated from electron backscattered diffraction (EBSD) analyses that single-crystal architecture is created in ferroelectric $Sm_{0.5}La_{0.5}BGeO_5$ crystal lines patterned by laser irradiations in a glass with the composition of $Sm_{0.5}La_{0.5}BGeO_5$.

So far, dots and lines consisting of crystals have been patterned in glasses by laser irradiations, i.e., zero-dimensional dot and one-dimensional line patterning [1–20]. From a viewpoint of practical device applications for laser-patterned crystals, it is of interest and importance to pattern two-dimensional planar crystals, i.e., two-dimensional patterning. Here, the term of two-dimensional patterning is defined as the patterning of crystals with planar shapes such as square and circle. There have been, however, few reports on the patterning of two-dimensional planar crystals on the glass surface using laser-induced crystallization techniques [21,22]. Very recently, Honma and Komatsu [21] succeeded in patterning two-dimensional planar $LiNbO_3$ (LN) crystal architectures on the surface of Li_2O–Nb_2O_5–B_2O_3–SiO_2 glass by continuous wave (cw) Yb:YVO_4 fiber laser (wavelength: $\lambda=1080$ nm) irradiations and demonstrated that the *c*-axis orientation of LN crystals is established along the laser scanning direction. Suzuki et al. [22] reported the pattering of two-dimensional planar β′-$(Gd,Sm)_2(MoO_4)_3$ crystals by laser irradiations. However, the orientation behavior of β′-$(Gd,Sm)_2(MoO_4)_3$ crystals has not been clarified well, because β′-$(Gd,Sm)_2(MoO_4)_3$ crystals patterned by laser irradiations have a unique periodic domain structure giving different refractive indices and thus homogeneous two-dimensional planar crystals have not been obtained. In order to clarify the orientation of crystals in two-dimensional crystal patterning, the patterning of other crystals having more simple crystal structure is desired.

In this study, we applied the laser-induced crystallization technique (rare-earth atom heat processing method) [3,5–7] to pattern two-dimensional planar crystals consisting of β-BaB_2O_4 crystals (β-BBO) on the surface of Sm_2O_3–BaO–B_2O_3 glass, in which cw Yb:YVO_4 fiber lasers with $\lambda=1080$ nm were irradiated onto the glass surface and scanned continuously with small steps between laser irradiated areas. β-BBO developed by Chen et al. [23] is one of the most important nonlinear optical crystals in laser optics, and numerous studies on the fabrication and properties of β-BBO with different morphologies have been reported so far. It is, therefore, considered that the laser patterning of two-dimensional planar β-BBO crystals with high orientation would give a great contribution on the science and technology of optical

* Corresponding author. Fax: +81 258 47 9300.
E-mail address: komatsu@mst.nagaokaut.ac.jp (T. Komatsu).

0022-4596/$ - see front matter © 2011 Elsevier Inc. All rights reserved.
doi:10.1016/j.jssc.2011.11.005

functional materials. The patterning of β-BBO crystal dots and lines by laser irradiation in $BaO–B_2O_3$ based glasses have been reported by Miura et al. [1], Avanshi et al. [9], and the present authors group [5,24,25], but there has been no report on the patterning of two-dimensional planar β-BBO crystals.

2. Experimental

A glass with the composition of $8Sm_2O_3–42BaO–50B_2O_3$ (mol%) was prepared using a conventional melt quenching technique. Commercial powders of reagent grade Sm_2O_3, $BaCO_3$, and H_3BO_3 were melted in a platinum crucible at 1200 °C for 40 min in an electric furnace. Melts were poured on to an iron plate and pressed to a thickness of ~1.5 mm by another iron plate. Glass transition, T_g, and crystallization onset, T_x, temperatures were determined using differential thermal analysis (DTA) at a heating rate of 10 K/min. The quenched glasses were annealed at T_g for 30 min to release internal stresses.

Glasses were mechanically polished to a mirror finish with CeO_2 powders. The glass surface was irradiated by cw Yb:YVO_4 fiber laser (beam shape: single mode and ±1 nm bandwidth) with $\lambda=1080$ nm using objective lens (magnification: 50 times, numerical aperture: NA=0.8). The diameter of laser spot size was 2–3 μm. Plate-shaped glasses were put on the stage and mechanically moved during laser irradiations to construct two-dimensional planar crystals. Laser-irradiated parts were observed with a polarization optical microscope (POM) and a confocal scanning laser microscope (CSLM) (Olympus-OLS 3000). The crystalline phase in the laser-irradiated part was examined from micro-Raman scattering spectrum measurements (Tokyo Instruments Co., Nanofinder; Ar^+ laser with $\lambda=488$ nm). Second harmonic generations (SHGs) were measured with a Maker fringe technique, in which a Q-switched Nd:YAG (yttrium aluminum garnet) laser with $\lambda=1064$ nm was used as the incident light and second harmonic (SH) light ($\lambda=532$ nm) was detected.

3. Results and discussion

The melt-quenched sample of $8Sm_2O_3–42BaO–50B_2O_3$ (mol%) prepared in this study showed only a halo pattern in the X-ray diffraction analysis, and the endothermic peak due to the glass transition and exothermic peaks due to the crystallization were observed in the DTA curve. The values of the glass transition and the crystallization peak temperatures were determined to be $T_g=566$ °C and $T_p=681$ °C, respectively. In this study, $8Sm_2O_3–42BaO–50B_2O_3$ glass is designated as SBB glass. It was determined from an optical absorption spectrum that the optical absorption coefficient (α: at room temperature) at $\lambda=1080$ nm (Yb:YVO4 laser) for SBB glass is $\alpha=10.1\ cm^{-1}$. It is known that Sm^{3+} ions give an optical absorption band at around 1080 nm due to the *f–f* transitions between $^6H_{5/2}$ and $^6F_{9/2}$. It was confirmed that the crystalline phase formed by heat treatment in an electric furnace is identified to be only the β-BaB_2O_4 crystalline phase (ICDD# 85-0914) [5,24,25].

3.1. Growth orientation of β-BBO crystals in discrete line

Prior to the patterning of two-dimensional planar β-BBO crystals, we first patterned discrete β-BBO crystal lines and clarified the feature of the crystal growth direction. In the previous paper [5], the discrete lines consisting of β-BBO single crystals have been patterned on the glass surface of $10Sm_2O_3–40BaO–50B_2O_3$ and $10Dy_2O_3–45BaO–55B_2O_3$ by irradiations of cw Nd:YAG laser with $\lambda=1064$ nm. Because phenomena (e.g., structural relaxation, nucleation and crystal growth in crystallization) taking place in the laser-irradiated region in glass depend on laser irradiation conditions (laser type, power, scanning speed) and properties of a given glass, it would be necessary to confirm the quality of β-BBO crystal lines patterned by cw Yb:YVO_4 fiber laser ($\lambda=1080$ nm) in the present glass of SBB. The CSLM photograph for the discrete line patterned by cw Yb:YVO_4 fiber laser irradiations with a laser power of $P=0.80$ W and a laser scanning speed $S=4$ μm/s is shown in Fig. 1. The bump with a height of 0.4 μm and a width of 5 μm is observed in the laser-irradiated part.

The azimuthal dependence of SHG signals for the discrete line (Fig. 1) is shown in Fig. 2, in which the measurements were carried out in the configuration of H–H. The notation of H–H means that the linearly polarized electric field of the incident laser is parallel to the electric field of SH waves in the measurements. Furthermore, the rotation angles of 0° and 180° correspond to the configuration that the polarized electric field of the incident laser is parallel to the line growth direction. The maximum SH intensities are observed at the rotation angles of ~0° and ~180°, the minimum intensities are located at ~90° and 270°. These profiles represent the two-fold angular dependence in the rotation and indicate the high orientation of β-BBO crystals in the discrete line patterned by cw Yb:YVO_4 fiber laser irradiations.

The linearly polarized micro-Raman scattering spectra at room temperature for the line are shown in Fig. 3. In the measurements,

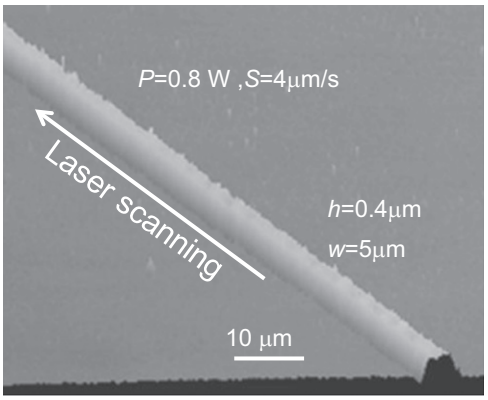

Fig. 1. CSLM photograph for the sample obtained by laser irradiations. The laser power and scanning speed were $P=0.8$ W and $S=4$ μm/s, respectively.

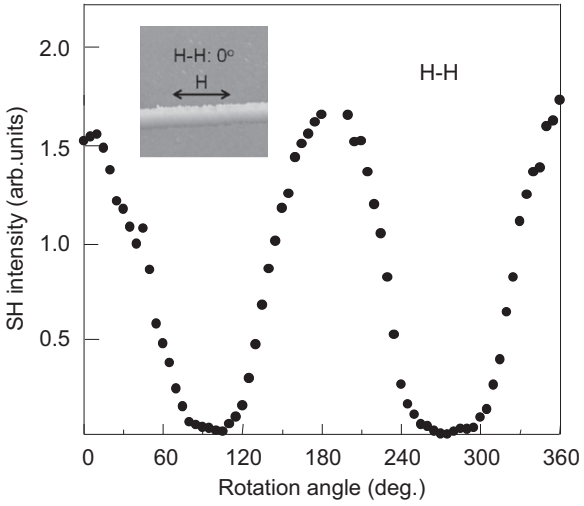

Fig. 2. Azimuthal dependence of SH intensities for the discrete line patterned by laser irradiations. The notations of H–H means that the polarized electric field of the incident laser is parallel to the electric field of SH waves in the measurement.

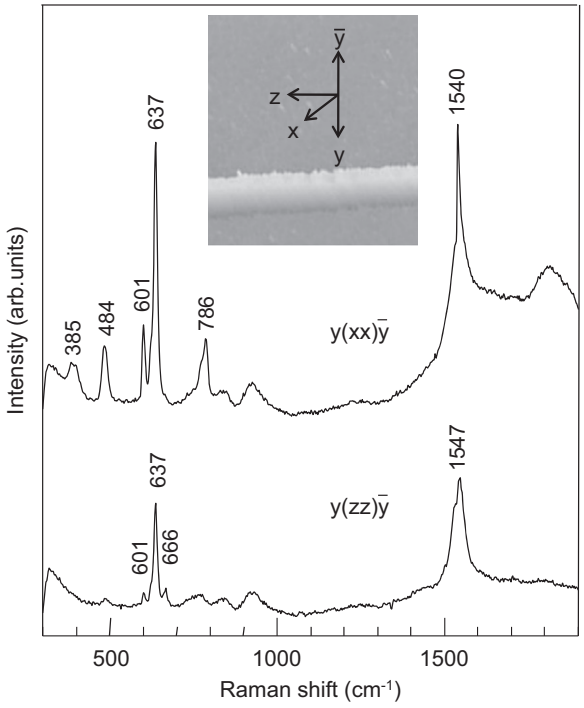

Fig. 3. Linearly polarized micro-Raman scattering spectra at room temperature for the discrete line patterned by laser irradiations. The configuration in the measurement is shown in the figure, and the direction of *z*-axis corresponds to the line growth direction.

the direction of *z*-axis in the configuration corresponds to the line growth direction, i.e., laser scanning direction. For instance, the configuration of $y(zz)\bar{y}$ means that incident laser introduced from *y*-axis direction has a polarization (electric vector) of *z*-axis and Raman light with polarization of *z*-axis is detected from $-y$ direction (backscattering arrangement). Several sharp peaks are observed at 385, 484, 601, 637, 668, 786, 1540 cm^{-1} in the configuration of $y(xx)\bar{y}$. The structure of β-BBO is formed by Ba^{2+} ions and planar $[B_3O_6]^{3-}$ anionic hexagonal rings, and the peaks shown in Fig. 3 are attributed to the characteristic vibrations of $[B_3O_6]^{3-}$ rings. In particular, the vibrations at 637 cm^{-1} with a strong intensity, 786 cm^{-1}, and 1540 cm^{-1} are assigned to the intra-ring B–O–B angle bending, the intra-ring B–O stretching, and the extra-ring B–O stretching, respectively [25]. It is noted that the peak intensity at 637 cm^{-1} in $y(xx)\bar{y}$ is larger than that in $y(zz)\bar{y}$. Furthermore, some peaks at 385, 484, and 786 cm^{-1} observed in $y(xx)\bar{y}$ are not detected in the configuration of $y(zz)\bar{y}$. These results shown in Fig. 3 also indicate a high orientation of β-BBO crystals in the discrete line. Because the polarized Raman scattering spectra shown in Fig. 2 correspond to those for y-cut β-BBO single crystals [5,25], it is proposed that the growth direction of β-BBO crystals along laser scanning direction is the *c*-axis.

3.2. Patterning of planar β-BBO crystals and growth direction

Our methodology for the patterning of planar β-BBO crystals by laser irradiations is to irradiate lasers with small steps between laser irradiated areas. That is, a forthcoming laser irradiation is overlapped to the former laser-irradiated part. In this study, the different step widths of 1 and 0.5 μm were applied.

First, the laser scanning was repeated with a step of 1 μm between the lines using the condition of $P=0.8$ W and $S=8$ μm/s, and the POM and CSLM photographs for the sample obtained are shown in Fig. 4. The laser scanning direction and step direction

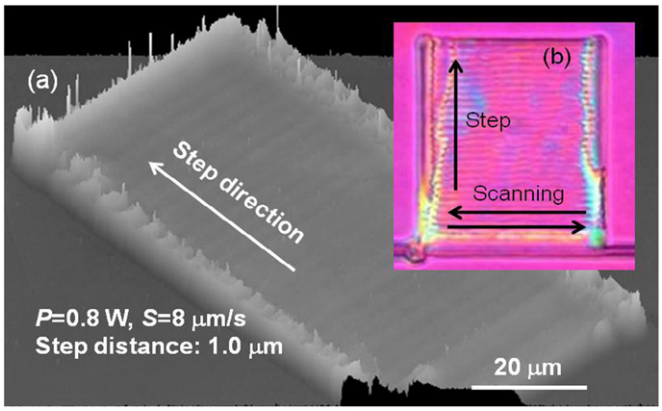

Fig. 4. CSLM (a) and POM (b) photographs for the sample obtained by laser irradiations. The laser power, scanning speed, and step distance were $P=0.8$ W, $S=4$ μm/s, and 1 μm, respectively. The laser scanning direction and step direction are shown in the figure.

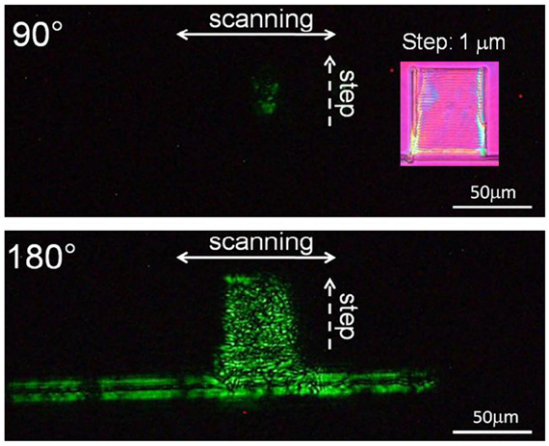

Fig. 5. SH wave images (the intensity of green light with $\lambda=532$ nm) observed in the configuration of H–H for the sample obtained by laser irradiations (Fig. 4) with $P=0.8$ W, $S=4$ μm/s, and the step distance of 1 μm. The angle of 90° and 180° corresponds to the angle between the linearly polarized direction of incident laser for SHG measurements and the laser scanning direction for the pattering of β-BBO crystals.

are indicated in the figure. The bumps are observed in the laser-irradiated parts, as similar to the discrete lines (Fig. 1). It is seen that this step of 1 μm induces the overlapping of laser irradiated parts. But, the surface of the sample is not smooth, implying that the overlapping is not sufficient. In the POM photograph (top view) for the sample (step: 1 μm), the center part gives a homogeneous color, but the color of the edge part is different from that of the center part. At the edge part, the laser scanning direction changes (reverse). That is, the edge part is the turning point for the laser scanning. In other words, it is expected that the crystallization behavior of β-BBO at the edge part would be different from that in the center part.

The SH wave images (the intensity of green light with $\lambda=532$ nm) observed in the configuration of H–H for the sample (Fig. 4) are shown in Fig. 5. The angle of 90° and 180° corresponds to the angle between the linearly polarized direction of incident laser for SHG measurements and the laser scanning direction for the pattering of β-BBO crystals. At the angle of 180°, the SHG is observed in the whole part of the overlapped laser-irradiated part. On the other hand, at the angle of 90°, any clear SHG is not observed in the whole part. These results indicate that β-BBO crystals patterned by laser irradiations with a step of 1 μm are

highly oriented. Furthermore, it is concluded that the orientation of β-BBO crystals in the overlapped laser-irradiated part is the same as that (Fig. 2) in the discrete line.

The laser scanning was repeated with a step of 0.5 μm between the lines using the condition of P=0.8 W and S=8 μm/s, and the POM and CSLM photographs for the sample obtained are shown in Fig. 6. It is found that the surface of the overlapped laser-irradiated part is more smooth compared with the case of the step of 1 μm (Fig. 4), suggesting more well overlapping of laser-irradiated parts. The POM photograph (top view) also indicates the formation of the smooth surface in the overlapped laser-irradiated part. The SH wave images observed in the configuration of H–H for the sample (Fig. 6) are shown in Fig. 7. At the angle of 180°, SHGs are observed in the initial line, but not observed in the overlapped laser-irradiated part. Contrary, at the angle of 90°, SHGs are observed only in the overlapped laser-irradiated part. That is, in the laser irradiation with a step of 0.5 μm, it is concluded that the orientation of β-BBO crystals in the overlapped laser-irradiated part is different from that in the discrete line.

In order to confirm more clearly the unique orientation observed in the overlapped laser-irradiated part with a step of 0.5 μm (Figs. 6 and 7), the azimuthal dependence of SHG signals for the overlapped laser-irradiated part was measured, and the result is shown in Fig. 8. The measurements were carried out in the configuration of H–H as similar to the case of the discrete line shown in Fig. 2. The maximum SH intensities are observed at the rotation angles of ~90° and ~270°, and the minimum intensities are located at 0° and ~180°. These results are largely different from those observed for the discrete line shown in Fig. 2. Furthermore, the appearance of the two-fold angular dependence shown in Fig. 8 demonstrates that β-BBO crystals in the overlapped laser-irradiated part with a step of 0.5 μm are highly oriented. In this paper, we propose that such β-BBO crystals patterned by laser irradiations are "*two-dimensional planar β-BBO crystals*". The azimuthal dependence of SHG signals has been observed for the two-dimensional planar crystals even in the case of $LiNbO_3$ and β′-$(Gd,Sm)_2(MoO_4)_3$ [21,22]. It is of importance to evaluate SHG efficiencies of two-dimensional planar crystals patterned by laser irradiations for practical applications. Such a study is now under consideration.

The linearly polarized micro-Raman scattering spectra at room temperature for the two-dimensional planar β-BBO crystals (Fig. 6) were measured, and the results are shown in Fig. 9. In the measurements, the directions of z-axis and x-axis in the configuration correspond to the laser scanning direction and step direction, respectively, as indicated in Fig. 9. Several sharp peaks assigned to the Raman bands in β-BBO crystals are observed. It is also found that the intensity of Raman bands depends largely on the configuration of $y(zz)\bar{y}$ and$y(xx)\bar{y}$, indicating the orientation of β-BBO crystals in the overlapped laser-irradiated part. Furthermore, it is noted that the Raman spectrum (Fig. 9) observed for the configuration of $y(zz)\bar{y}$ in the planar β-BBO crystals is almost the same as that for the configuration of $y(xx)\bar{y}$ in the β-BBO discrete line (Fig. 3). And, the Raman spectrum for the configuration of $y(xx)\bar{y}$ in the planar β-BBO crystals corresponds to that for the configuration of $y(zz)\bar{y}$ in the β-BBO discrete line. These results suggest that β-BBO crystals in the overlapped laser-irradiated part are highly oriented and the c-axis direction of β-BBO crystals is perpendicular to the laser scanning direction or parallel to the laser step direction.

In order to examine the orientation of β-BBO crystals in the overlapped laser-irradiated part (Fig. 6) more in detail, two-dimensional micro-Raman scattering spectra (imaging) for the

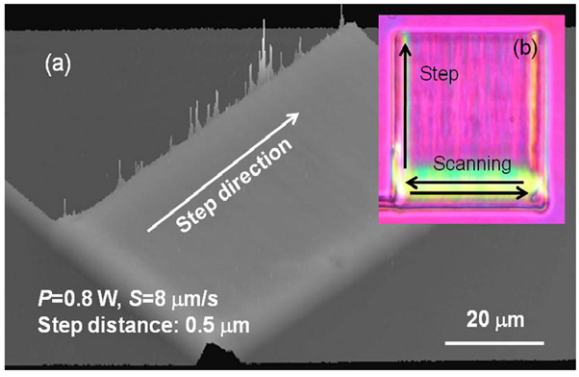

Fig. 6. CSLM (a) and POM (b) photographs for the sample obtained by laser irradiations. The laser power, scanning speed, and step distance were P=0.8 W, S=4 μm/s, and 0.5 μm, respectively. The laser scanning direction and step direction are shown in the figure.

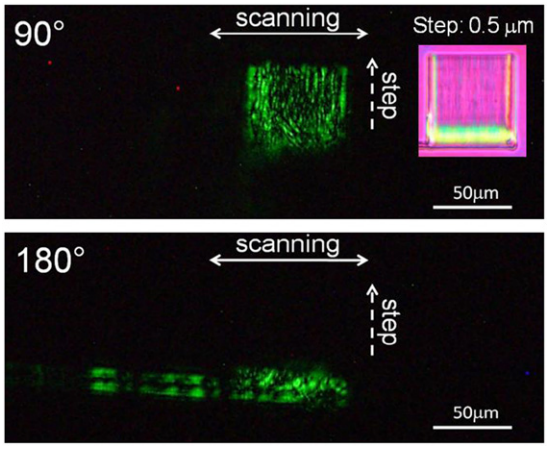

Fig. 7. SH wave images (the intensity of green light with λ=532 nm) observed in the configuration of H–H for the sample obtained by laser irradiations (Fig. 6) with P=0.8 W, S=4 μm/s, and the step distance of 0.5 μm. The angle of 90° and 180° corresponds to the angle between the linearly polarized direction of incident laser for SHG measurements and the laser scanning direction for the pattering of β-BBO crystals.

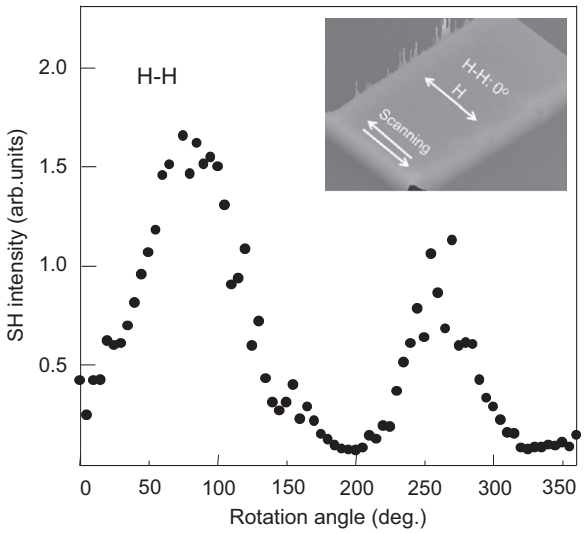

Fig. 8. Azimuthal dependence of SH intensities for the two-dimensional planar β-BBO crystals obtained by laser irradiations. The laser power, scanning speed, and step distance were P=0.8 W, S=4 μm/s, and 0.5 μm, respectively. The notations of H–H means that the polarized electric field of the incident laser is parallel to the electric field of SH waves in the measurement.

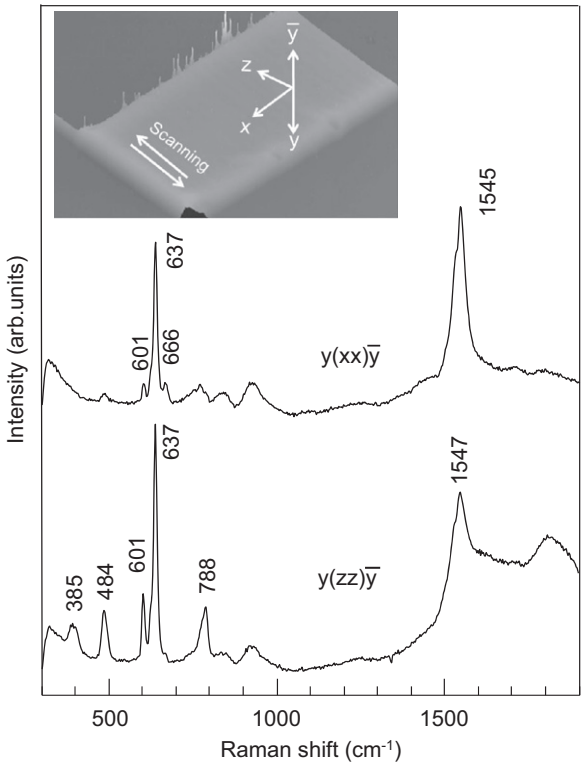

Fig. 9. Linearly polarized micro-Raman scattering spectra at room temperature for the two-dimensional planar β-BBO crystals obtained by laser irradiations (Fig. 6). The configuration in the measurement is shown in the figure, and the direction of *z*-axis corresponds to the laser scanning direction.

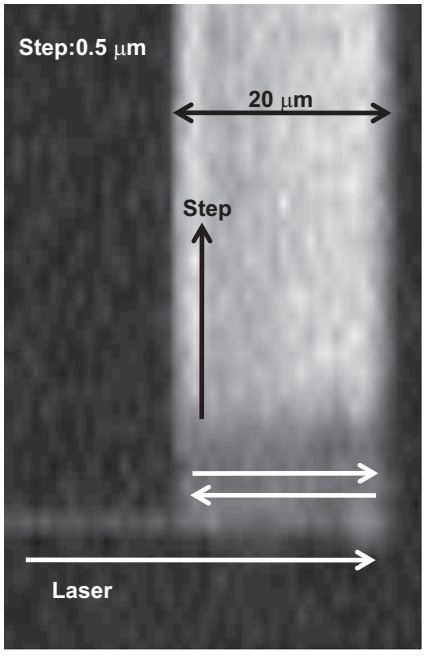

Fig. 10. Two-dimensional micro-Raman scattering spectra (imaging) at room temperature for the configuration of $y(zz)\bar{y}$. The intensity of the peak at 637 cm^{-1} is focused, and the white color means the strong intensity of the Raman peak at 637 cm^{-1}.

configuration of $y(zz)\bar{y}$ were measured at room temperature. The results are shown in Fig. 10. In this experiment, the intensity of the peak at 637 cm^{-1} is focused, and the white color means the strong intensity of the Raman peak at 637 cm^{-1}. It is seen that the intensity of the white color is small in the initial laser-irradiated part (discrete line) and also in the overlapped (repeated) laser-irradiated part of about 10 μm at the beginning (near the discrete line). However, it is found that the intensity of the white color increases gradually and becomes almost constant with increasing step distance. These results indicate that the orientation of β-BBO crystals changes gradually. The schematic model for the *c*-axis direction of β-BBO crystals in the overlapped laser-irradiated part is shown in Fig. 11.

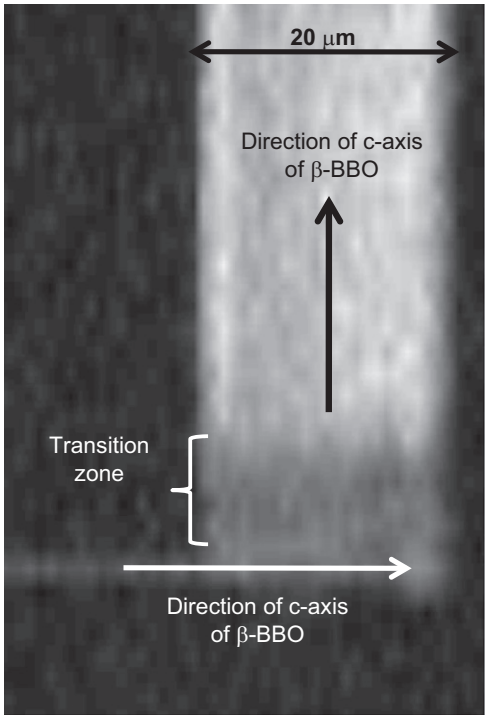

Fig. 11. Schematic model for the *c*-axis direction of β-BBO crystals in the two-dimensional planar β-BBO crystals patterned by overlapped laser irradiations (Fig. 10).

The melting temperature of β-BBO crystals is known to be 1095 °C. At this moment, the temperature of the laser-irradiated region (Yb:YVO_4 laser (λ=1080 nm), P=0.8 W and S=8 μm/s) is not measured, but it is obvious that the temperature is higher than the crystallization temperature (T_p=681 °C) of $8Sm_2O_3$–$42BaO$–$50B_2O_3$ (mol%) glass examined in this study. As can be seen in Fig. 6, any damage such as melting or ablation is not observed at the surface of the overlapped laser-irradiated part, and thus, it is expected that the temperature would not be higher than the melting temperature (1095 °C) of β-BBO crystals. In the overlapped laser-irradiated part, therefore, it is considered that initial β-BBO crystals patterned by laser irradiations are not melted, but melt (i.e., super-cooled liquid) is created at the side (i.e., the glass part) of initial β-BBO crystals. Considering the *c*-axis direction of β-BBO crystals in the overlapped laser-irradiated part shown in Fig. 11, it is concluded that the interface between the initial β-BBO crystals and melt might have an important role for the growth and orientation of new (forthcoming) β-BBO crystals. In other words, the initial β-BBO crystals might act as nucleation sites for the growth of new β-BBO crystals.

4. Conclusions

The laser-induced crystallization method was applied to pattern two-dimensional planar β-BaB_2O_4 crystals on the surface of $8Sm_2O_3$–$42BaO$–$50B_2O_3$ glass. By scanning Yb:YVO_4 fiber lasers

(wavelength: 1080 nm) continuously with a small step (0.5 μm) between laser irradiated areas, homogeneous planar β-BaB_2O_4 crystals were patterned successfully, and a preferential growth orientation of β-BaB_2O_4 crystals was confirmed from linearly polarized micro-Raman scattering spectrum and second harmonic intensity measurements. It was found that the crystal growth direction is perpendicular to the laser scanning direction. This relation was different from the behavior in discrete crystal line patterning. The present study proposes the possibility of the control of crystal growth direction in laser-induced crystallization in glasses.

Acknowledgment

This work was supported from the Grant-in-Aid for Scientific Research from the Ministry of Education, Science, Sports, Culture and Technology, Japan, and by Program for High Reliable Materials Design and Manufacturing in Nagaoka University of Technology.

References

[1] K. Miura, J. Qiu, T. Mitsuya, K. Hirao, Opt. Lett. 25 (2000) 408.
[2] R. Sato, Y. Benino, T. Fujiwara, T. Komatsu, J. Non-Cryst. Solids 289 (2001) 228.
[3] T. Honma, Y. Benino, T. Fujiwara, T. Komatsu, R. Sato, Appl. Phys. Lett. 82 (2003) 892.
[4] M. Nogami, A. Ohno, H. You, Phys. Rev. B 68 (2003) 104204.
[5] T. Honma, Y. Benino, T. Fujiwara, T. Komatsu, R. Sato, Appl. Phys. Lett. 83 (2003) 2796.
[6] T. Honma, Y. Benino, T. Fujiwara, T. Komatsu, Appl. Phys. Lett. 88 (2006) 231105.
[7] T. Komatsu, R. Ihara, T. Honma, Y. Benino, R. Sato, H.G. Kim, T. Fujiwara, J. Am. Ceram. Soc. 90 (2007) 699.
[8] B. Franta, T. Williams, C. Faris, S. Feller, M. Affatigato, Phys. Chem. Glasses: Eur. J. Glass Sci. Technol. B 48 (2007) 357.
[9] W. Avansi, V.R. Mastelaro, M.R.B. Andreeta, J. Non-Cryst. Solids 354 (2008) 279.
[10] P. Gupta, H. Jain, D.B. Williams, T. Honma, Y. Benino, T. Komatsu, J. Am. Ceram. Soc. 91 (2008) 110.
[11] M. Kusatsugu, M. Kanno, T. Honma, T. Komatsu, J. Solid State Chem. 181 (2008) 1176.
[12] Y. Tsukada, T. Honma, T. Komatsu, Appl. Phys. Lett. 94 (2009) 059901.
[13] T. Honma, T. Komatsu, D. Zhao, H. Jain, IOP Conf. Series: Mater. Sci. Eng. 1 (2009) 012006.
[14] V.N. Sigaev, E.A. Alieva, S.V. Lotarev, N.M. Lepekhin, Y.S. Priseko, A.V. Rasstanaev, Glass Phys. Chem. 35 (2009) 13.
[15] M. Kanno, T. Honma, T. Komatsu, J. Am. Ceram. Soc. 92 (2009) 825.
[16] L.L. Martin, P. Haro-Gonzalez, I.R. Martin, D. Puerto, J. Solis, J.M. Caceres, N.E. Capuj, Opt. Mater. 33 (2010) 186.
[17] A. Stone, M. Sakakura, Y. Shimotsuma, G. Stone, P. Gupta, K. Miura, K. Hirao, V. Dierolf, H. Jain, J. Non-Cryst. Solids 356 (2010) 3059.
[18] F. Suzuki, T. Honma, T. Komatsu, J. Solid State Chem. 183 (2010) 909.
[19] K. Kioka, T. Honma, T. Komatsu, Opt. Mater. 33 (2011) 1203.
[20] T. Komatsu, K. Koshiba, T. Honma, J. Solid State Chem. 184 (2011) 411.
[21] T. Honma, T. Komatsu, Opt. Express 18 (2010) 8019.
[22] F. Suzuki, T. Honma, T. Komatsu, Mater. Chem. Phys. 125 (2011) 377.
[23] C. Chen, Y. Wu, R. Li, J. Cryst. Growth 99 (1990) 790.
[24] H. Tanaka, T. Honma, Y. Benino, T. Fujiwara, T. Komatsu, J. Phys. Chem. Solids 64 (2003) 1179.
[25] T. Honma, Y. Benino, T. Fujiwara, R. Sato, T. Komatsu, J. Phys. Chem. Solids 65 (2004) 1705.